



Title	Surface morphology of a glow discharge electrode in a solution
Author(s)	Saito, Genki; Hosokai, Sou; Tsubota, Masakatsu et al.
Citation	Journal of Applied Physics, 112(1), 013306 https://doi.org/10.1063/1.4732076
Issue Date	2012-07-01
Doc URL	https://hdl.handle.net/2115/49730
Rights	Copyright 2012 American Institute of Physics. This article may be downloaded for personal use only. Any other use requires prior permission of the author and the American Institute of Physics. The following article appeared in J. Appl. Phys. 112, 013306(2012) and may be found at https://dx.doi.org/10.1063/1.4732076
Type	journal article
File Information	JAP_112(1)_013306.pdf





Surface morphology of a glow discharge electrode in a solution

Genki Saito, Sou Hosokai, Masakatsu Tsubota, and Tomohiro Akiyama

Citation: *J. Appl. Phys.* **112**, 013306 (2012); doi: 10.1063/1.4732076

View online: <http://dx.doi.org/10.1063/1.4732076>

View Table of Contents: <http://jap.aip.org/resource/1/JAPIAU/v112/i1>

Published by the [American Institute of Physics](#).

Related Articles

Delineating local electromigration for nanoscale probing of lithium ion intercalation and extraction by electrochemical strain microscopy

Appl. Phys. Lett. **101**, 063901 (2012)

Phase-field modeling of three-phase electrode microstructures in solid oxide fuel cells

Appl. Phys. Lett. **101**, 033909 (2012)

Dynamic modelling and simulation of a polymer electrolyte membrane fuel cell used in vehicle considering heat transfer effects

J. Renewable Sustainable Energy **4**, 043107 (2012)

Colloidal electroconvection in a thin horizontal cell. III. Interfacial and transient patterns on electrodes

J. Chem. Phys. **137**, 014504 (2012)

Use of magnetite as anode for electrolysis of water

J. Appl. Phys. **111**, 124911 (2012)

Additional information on *J. Appl. Phys.*

Journal Homepage: <http://jap.aip.org/>

Journal Information: http://jap.aip.org/about/about_the_journal

Top downloads: http://jap.aip.org/features/most_downloaded

Information for Authors: <http://jap.aip.org/authors>

ADVERTISEMENT

World's Ultimate AFM Experience the Speed & Resolution



The fastest AFM on the planet is now simply the best AFM in the world

[CLICK TO REQUEST INFO](#)

Surface morphology of a glow discharge electrode in a solution

Genki Saito, Sou Hosokai, Masakatsu Tsubota, and Tomohiro Akiyama^{a)}

Center for Advanced Research of Energy and Materials, Hokkaido University, Sapporo 060-8628, Japan

(Received 14 March 2012; accepted 31 May 2012; published online 9 July 2012)

This paper describes the surface morphology of a glow discharge electrode in a solution. In the experiments detailed in the paper, the effects of electrolysis time, solution temperature, voltage, electrolyte concentration, and surface area on the size of nanoparticles formed and their amount of nanoparticles produced were examined to study the surface morphologies of the electrodes. The results demonstrated that the amount of nanoparticles produced increased proportionally with the electrolysis time and current. When the voltages were below 140 V, surfaces with nanoparticles attached, called “Particles” type surfaces, were formed on the electrode. These surfaces changed and displayed ripples, turning into “Ripple” type surfaces, and the nanoparticle sizes increased with an increase in the amount of nanoparticles produced. In contrast, at voltages over 160 V, the surfaces of the electrodes were either “Random” or “Hole” type and the particle sizes were constant at different amount of nanoparticles produced. © 2012 American Institute of Physics. [<http://dx.doi.org/10.1063/1.4732076>]

I. INTRODUCTION

When a high direct current (DC) voltage is applied to a conductive electrode in a solution, a plasma layer is generated at the interface between the electrode and the solution. The formation of the plasma layer is due to the heating of the solution near the electrode. The electrode under such conditions was named “a glow discharge electrode” by Hickling and Ingram,¹ who studied light emission from such electrodes. They performed a conventional electrolysis of water and increased the current by increasing the voltage from a low value. Since the heating of the solution due to electrical resistance was concentrated at the electrode/solution interface, the solution near the cathode heated to its boiling point and a gas layer containing hydrogen gas and steam was generated. If the voltage was sufficiently high, the gas layer formed a glow discharge plasma that was accompanied by light emission. The emission spectra of this radiation depended on the constituent elements of the electrolyte and electrode materials.^{2–4} A glow discharge electrode can be used for the synthesis of organic-inorganic superabsorbent composition⁵ and degradation of pollutants.⁶

Recently, a solution plasma was applied in the synthesis of nanoparticles.⁷ Gold nanoparticles were synthesized from the solution of HAuCl₄.^{8,9} Paulmier *et al.* report the synthesis of TiO₂ nanorods using contact glow discharge electrolysis.¹⁰ The nanoparticles of Ni, Ti, Ag, and Au were produced by the electrode dissolution during a solution plasma using a glow discharge electrode.¹¹ Previous reports indicate that this solution plasma produces not only metallic nanoparticles but also oxide nanoparticles such as ZnO (Ref. 12) and CuO.¹³ In addition, the size and composition of these nanoparticles can be controlled by changing the experimental conditions.^{14,15} This method for producing nanoparticles has many advantages: (1) it requires a simple experimental setup without the need for a vacuum chamber; (2) there is no need

to supply any gas; (3) a conductive electrode is used as the raw material, and harmful reductants or expensive agents are not required; and (4) it can be applied to any electrically conductive metal/alloy. To produce nanoparticles for various applications, control of the particle size and efficient production are essential. However, in spite of their importance, the parameters that are essential for controlling the formation of nanoparticles have not been well understood. Further, the relationship between the surface morphologies of the electrode and the experimental conditions has not been reported. The surface morphologies may be helpful in understanding the mechanism of nanoparticle formation. In this study, we investigated the surface morphology of a glow discharge electrode in a solution. In the experiments detailed in the paper, the effects of electrolysis time, solution temperature, voltage, electrolyte concentration, and surface area on the size of nanoparticles formed, and their amount of nanoparticles produced were examined to study the surface morphologies of the electrodes. Finally, key factors affecting the formation of nanoparticles were discussed carefully.

II. EXPERIMENTS

A. Experimental setup

As reported previously,¹³ the experimental setup consisted of two electrodes in a glass cell with a capacity of 300 ml. The cathode consisted of a Ni wire with a diameter of 1.0 mm and purity of more than 99.9 mass% (Kojundo chemical, Saitama, Japan) placed at the center of the glass cell. The upper and lower parts of the cathode were shielded by a quartz glass tube to keep the exposed length constant. The exposed portion functioned as the actual electrode. The anode consisted of a Pt wire with a length of 1000 mm, diameter of 0.5 mm, and purity of 99.98 mass% (Nilaco, Tokyo, Japan), and it was bent into a semicircular mesh. The distance between the electrodes was maintained at 30 mm. A glow discharge plasma was generated around the cathode and was maintained by applying a voltage using a direct current power

^{a)}E-mail: takiyama@eng.hokudai.ac.jp.

supply (ZX800H, Takasago, Tokyo, Japan). A NaOH solution was used as the electrolyte. The solution temperature was recorded every 5 s at a depth of 10 mm using a polymer-coated thermistor thermometer (Ondotori TR-71Ui, T&D, Nagano, Japan). The current and voltage were recorded every 2 s using a DC power supply.

B. Experimental conditions and procedure

The standard conditions were an electrolysis time of 60 min, voltage of 140 V, electrolyte concentration of 0.1 M, and exposed length of 10 mm without any agitation. To study the effect of the experimental conditions on the nanoparticles produced, we changed the electrolysis time, voltage, electrolyte concentration, solution temperature, and exposed length from their standard condition values. Table I (Appendix A) shows the experimental conditions. There were samples with the same experimental conditions, and these are denoted by asterisks. For example, the conditions for T-60, V-140, and I-10 were the same. To change the solution temperatures, the solutions were cooled or heated.

The experimental procedures are as follow. First, the solution was heated to $60 \pm 3^\circ\text{C}$. Then, the voltage was increased from 0.0 V to a preset level at a rate of $0.5 \text{ V}\cdot\text{s}^{-1}$, and the electrolysis voltage was maintained at the preset level for a preset time. In the case of changing the electrolyte concentration, we determined the rate of voltage increase needed to increase the voltage to the preset level in less than 300 s, because the prewarmed solution tended to cool down. Finally, after electrolysis, the products of the process were collected by centrifugation and washed with deionized water. Subsequently, the products were observed using an H-700 (Hitachi High-Technologies, Japan) transmission electron microscope. The collected particles were characterized by x-ray diffractometry (XRD) using a Miniflex II (Rigaku, Tokyo, Japan) diffractometer. The post-experiment cathode

wires were also observed using a JSM-7001F (JEOL, Tokyo, Japan) field-emission scanning electron microscope. The analytical method for calculating the mean diameter and analyzing the nanoparticle production is given in Appendix B.

III. RESULTS AND DISCUSSIONS

A. Electrolysis time

The electrolysis times were changed in the range from 1 to 360 min. Figure 1 shows the SEM images of the Ni wire after electrolysis for different electrolysis times. When the electrolysis times were less than 5 min, surfaces with particles attached to them were generated. We named such electrode surfaces “Particle” in order to categorize the different surface morphologies. After more than 30 min of electrolysis time, a rippled pattern was formed on the electrode surface, leading to what we have termed as a “Ripple” surface. A Ripple surface on the electrode during an electrode-melted solution plasma was first found, and it was probably caused by the sputtering effect. The orientation of these patterns was different at different areas of the electrode. Some areas did not have any Ripple patterns. These patterns probably depended on the crystal grains and the spacing of the ripple became wider with time. Figure 2(a) shows the relationship between the electrolysis time and nanoparticle production. This result indicates that the production increases in proportion to the electrolysis time. Figure 2(b) shows the plot of the mean diameter against the produced amount. The diameter of the nanoparticles produced in the early stages of the electrolysis is small. The particle size tends to increase with an increase in the production. This tendency was in agreement with the results of a previous paper in which the electrolysis time had been changed from 10 to 30 min.¹¹ From the XRD pattern, products were metallic nickel and didn't contain the nickel oxide (supplementary material available).²⁴ These

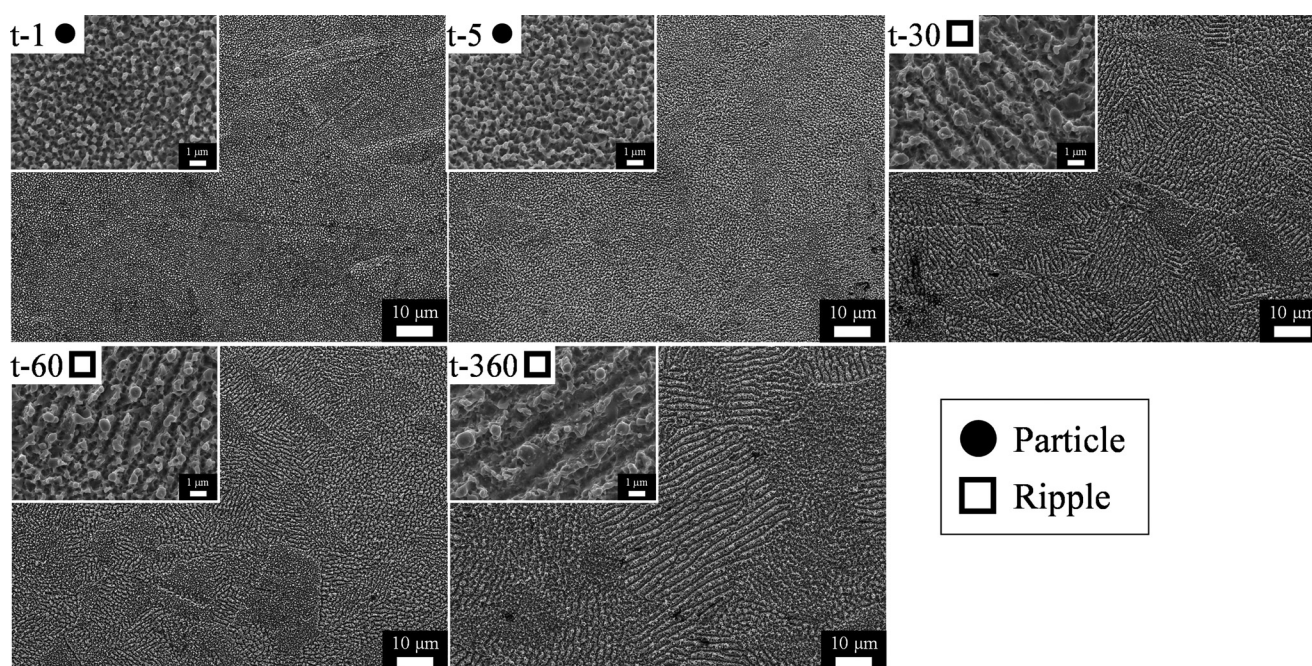


FIG. 1. SEM images of the Ni cathode wire observed after electrolysis for different electrolysis times.

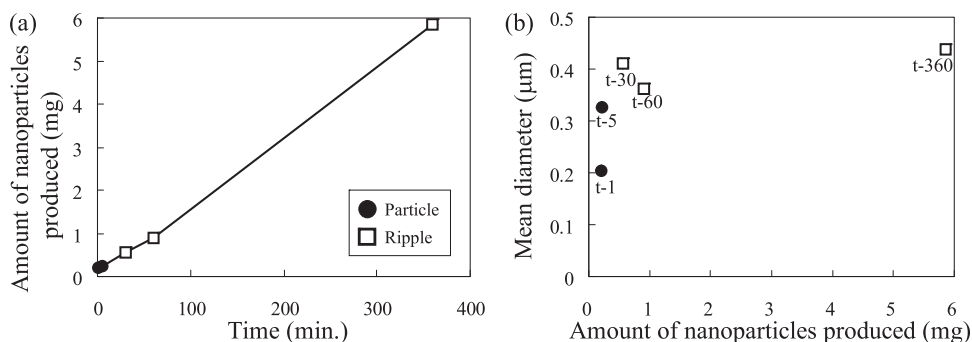


FIG. 2. (a) Plot of nanoparticle production against electrolysis time. The amounts of nanoparticles produced were calculated using the difference in the weight of the electrode before and after electrolysis. (b) Plot of mean diameter against the production at different electrolysis times. The mean diameter was measured from the TEM images.

results suggest that coarse particles were formed due to the rough surface. These results also suggested that the particle size depended on the amount of nanoparticles produced. Therefore, when the effects of the experimental conditions on the particle size are investigated, the total amount of nanoparticles produced should be carefully considered.

B. Electrolysis temperature

In order to control the solution temperatures, the electrolysis solution was either cooled or heated. For the T-1 condition, the electrolysis solution was cooled using ice water. In contrast, the electrolysis solution was heated with a heater for the T-5 condition. In the case of the T-3 condition, the electrolysis solution was cooled in the air. We measured the solution temperature at a certain point. There was a temperature distribution in the electrolysis solutions without agitation. Figure S4 shows the SEM images of the electrode surface after the experiment. The labels show the average temperatures of the solution during 60 min. For solution temperatures below 80 °C, the Ripple pattern was formed, similar to the pattern seen in the t-30, t-60, and t-360 conditions. At solution temperatures over 92 °C, the surfaces were Particle type. This difference in the surfaces can be explained by the nanoparticle production. Figure 3(a) shows a plot of the amount of nanoparticles produced against the mean diameter. The nanoparticle production decreased at high solution temperatures. The particle size was also decreased with a decrease in the nanoparticle production. Thus, in the case of less nanoparticle production, the electrode surface was Particle type. Figure 3(b) shows a plot of the mean diameter against the average current over 60 min. The high temperatures caused a decrease in the current because the gas layer completely covered the electrode and prevented the current from flowing. XRD patterns shown in Figure S7 indicate the solution temperature did not affect the composition of the products. From these results, it can be seen

that the production can be controlled by current and not by the solution temperature. A high current produces a large amount of particles. However, in the case labeled 64 °C, the production decreased despite the high current. This was because the electrolysis solution was too cold to fully form a plasma layer, and the electrolysis of water occurred at the interface between electrode surface and solution. This result also suggested that the suitable range for the solution temperature is from 69 to 80 °C.

C. Voltage

We investigated the effect of voltage on the particle size and production by changing the voltage from 80 to 200 V. The edge of the electrode was shielded by using a quartz glass tube. As reported previously, the edge-shield maintains a partial plasma region.¹⁵ After transition from partial-plasma region to full-plasma one, the products are oxidized and agglomerated. In the case of voltages from 80 to 120 V, the light emissions with a glow discharge were not clear. For the range from 140 to 180 V, the light emissions were observed, and the intensity of the light emission increased with an increase in the voltage. According to a video of the electrode surface taken by using a high-speed camera, the net area of plasma was quite small. Therefore, an increase in the light emission means that the net area of the discharge expands with an increase in the voltage. At 200 V, in spite of the use of the edge-shield, the discharge condition of the plasma transitioned to that of a full plasma, in which the particles were partially oxidized and agglomerated due to an increase in the surface temperature.¹⁵ The current was probably concentrated at the interface between the electrode and the quartz glass tube.

Figure 4 shows SEM images of the electrode after the experiments. When a voltage of 80 V was applied, an undulating surface was generated. This undulating surface is probably related to the crystal grains. Under the high temperature condition caused by the high voltage, the electrode surface

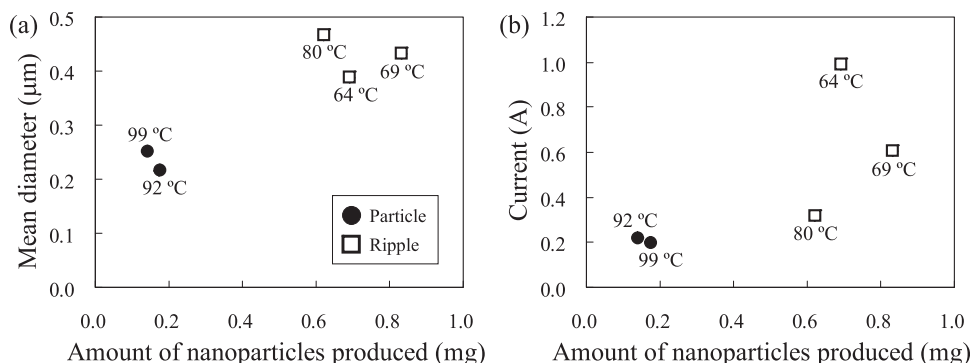


FIG. 3. (a) Plot of nanoparticle production against the mean diameter. The labels show the average temperatures of the solution over 60 min. (b) Plot of the mean diameter against the average current over 60 min.

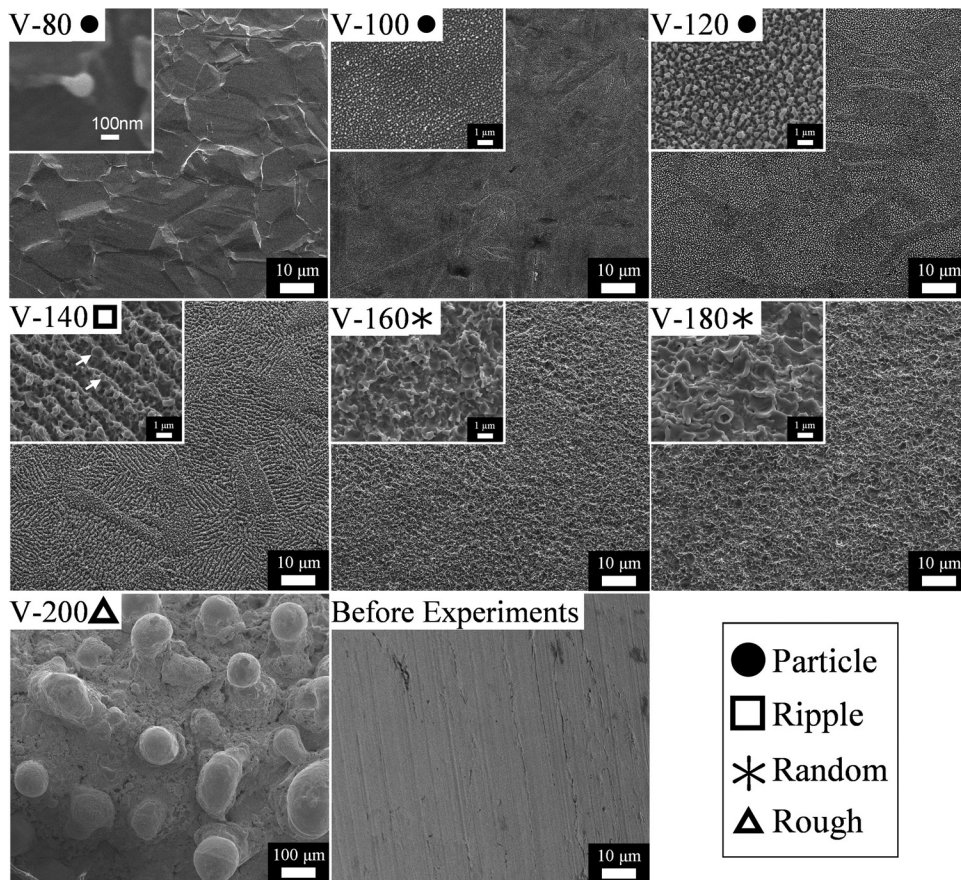


FIG. 4. SEM images of the Ni cathode wire observed after electrolysis at different voltages.

changed due to thermal expansion. Melted particles were also observed. For the range from 100 to 120 V, Particle type surfaces were formed. At 140 V, a Ripple type surface was formed. When the voltage was 160 V or 180 V, the surface had a random shape, which we have named “Random” for the purpose of classification. The high voltage caused a transition to the Random type surface. At 200 V, with a transition to full plasma, the electrode surface was quite rough. This is due to an increase in the surface temperature.

Figure 5(a) shows a plot of the nanoparticle production against the maintained current over 60 min at different voltages. In the range from 80 to 180 V, the current decreased with an increase in the voltage. As in the cases of changing the electrolysis time and solution temperature, described in Secs. III A and III B, the nanoparticle production increased with an increase in current. However, the high voltage values caused a low current and high production. The nanoparticles were formed by the concentration of the current.¹¹ Therefore, the nanoparticle production increases with an increase in the

current. High voltages accelerate the electrons and ions in the plasma sheath.¹⁶ The energy of the electrons increased owing to this acceleration under high voltage. Hence, the production increased with a decrease in the current at high voltages. The electric power needed to maintain the plasma tends to be a constant value. Based on this, the current was decreased with an increase in the voltage. We predict that the heat balance determines the electric power needed to maintain the plasma. When the solution is cooled, the electric current increases in order to make up for the heat loss, as shown in Sec. III B. Detailed information on the electric power settings under each condition is supplied as in the supplementary material.

Figure 5(b) shows a plot of the nanoparticle production against the mean diameter at different voltages. In the range from 80 to 120 V, a small amount of particles was obtained. This result indicated that the particles can be formed at 80 V. The nanoparticle production increased with an increase in the voltage. At voltages below 140 V, the mean diameter increased with an increase in the production. This is because

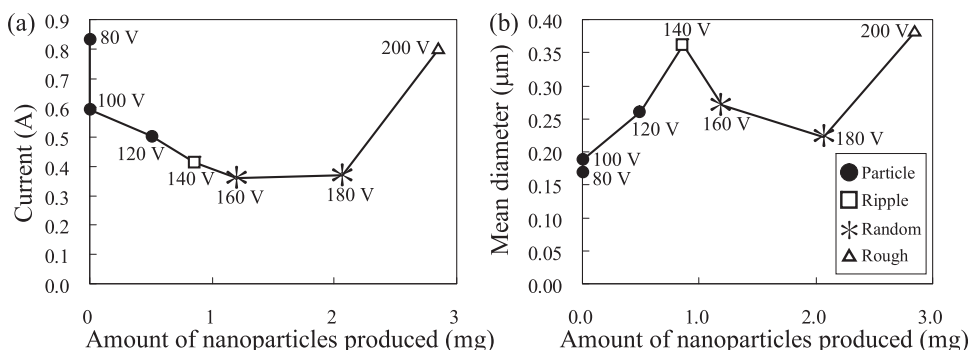


FIG. 5. (a) Plot of the average current over 60 min against the nanoparticle production. (b) Plot of the mean diameter at different applied voltages against the nanoparticle production.

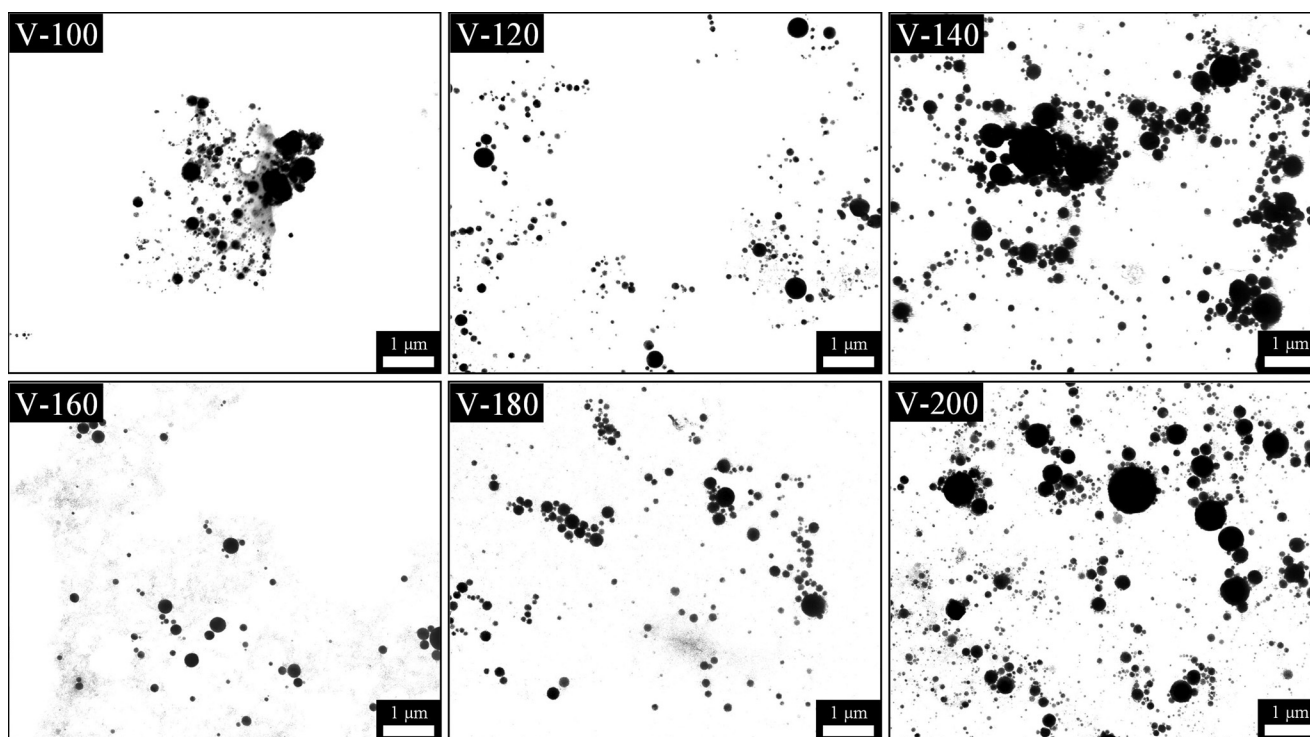


FIG. 6. TEM images of the products at different applied voltages.

the electrode surface became rough with an increase in the nanoparticle production, as was the case of in Sec. III A. However, in the range from 140 V to 180 V, the mean diameter decreased with an increase in the production. This result suggested that the voltage affected nanoparticle formation. In the case of the Ripple surface at 140 V, coarse particles were attached to the electrode surface (see arrows). We have also observed coarse particles in the products as shown in Fig. 6. The formation of these coarse particles increased the mean diameter. In contrast, the Random surface, which was formed at 160 and 180 V, does not have any coarse particles. This is the reason for the decrease in the particle size with an increase in the voltage. According to a previous report in which the voltage was changed from 100 to 160 V,¹¹ the particle size decreased with an increase in the voltage in the case of not only Ni but also other elements. At 200 V, the particle size increased because of the transition to a full plasma. Figure 7 summarizes the XRD patterns of the products. The full plasma at 200 V produced both metallic nickel and nickel oxide. This was exactly the same as the result obtained in the reported data.^{17,18} The measurement of the surface temperature of the electrode indicated that the temperature of full plasma was more than 2000 °C, in contrast, the temperature without transition to full plasma was less than 100 °C. The transition to full-plasma increased the surface temperature, and the products were oxidized as a result of high-temperature corrosion. The increase of the products size at the full plasma can be explained by the increase of a gas volume and a high temperature. According to the report,¹⁹ the size of the product produced by wire explosion is increased with increasing the gas volume over the cathode. Therefore, the large size of particles produced in the full plasma might be caused by the large volume of plasma zone.

D. Electrolyte concentration

As above mentioned in Sec. III C, the transition to a full-plasma due to an increase in the voltage happened at 200 V, in spite of the use of an edge-shield. The solution for using higher voltages without a transition to full-plasma is to use low electrolyte concentrations. When the concentration of the electrolysis solution is low, the current decreases due to an increase in the solution resistance. We previously reported that the use of low electrolyte concentrations could enable the use of high voltages without a transition to the full-plasma¹⁴ state. As a result, we successfully maintained a plasma condition without a transition to the full-plasma state at 600 V by using an electrolyte concentration of 0.001 M. The mean diameter decreased with a decrease in the production, as shown in Table II (Appendix C). During the change in the electrolyte concentration from 0.001 to 1.0 M, the highest nanoparticle production occurred at 180 V with an electrolyte concentration of 0.1 M. In the case of concentrations of 0.001 M and 1.0 M, the amounts of particles

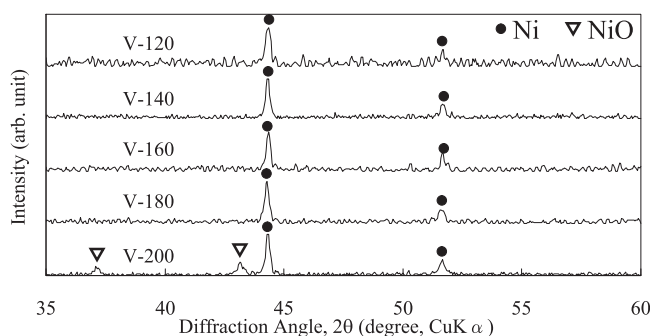


FIG. 7. XRD patterns of the products at different applied voltages.

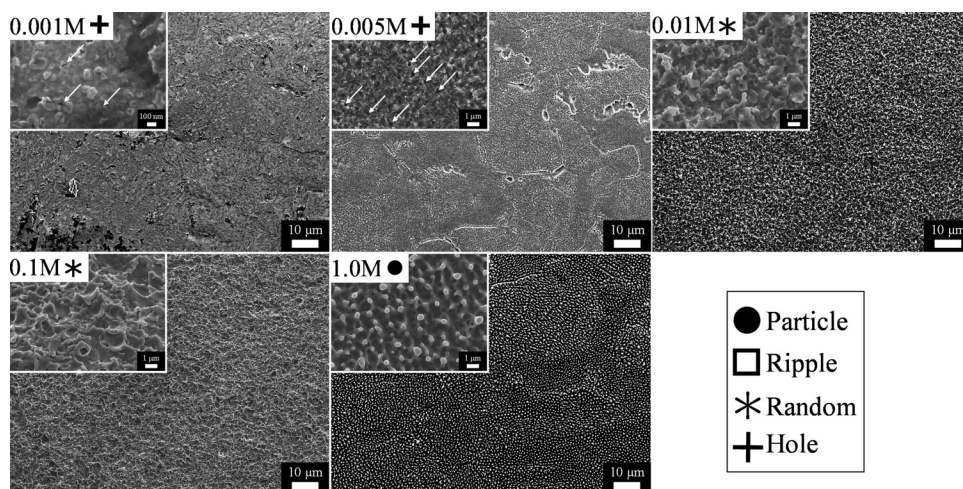


FIG. 8. SEM images of the Ni cathode wire observed after electrolysis at different concentrations.

produced were too small to be able to collect any. Figure 8 shows the SEM images of the electrode after this set of experiments. When the electrolyte concentrations were 0.001 M at 600 V and 0.005 M at 490 V, pores were formed on the electrode surface (arrows show), which we have named “Hole” for the purpose of classification. These pores on the electrode were also formed in other reported experiments.^{2,14} These surfaces were of the Random type in the case of 0.01 M and 0.1 M. At 1.0 M, the surface was of the Particles type. As mentioned in Sec. III C, the high voltage probably accelerates the charged particles such as electrons, Na^+ , and OH^- . There is a possibility that pores formed on the surface of the electrode at high voltage due to sputtering rather than the melting of the electrode surface.

E. Surface area

One way to increase the nanoparticle production is to extend the plasma area by using an electrode with a large surface area. The exposed length of the cathode wire was varied to 10 mm, 20 mm, and 30 mm. We predicted that the nanoparticle production would increase in proportion to the surface area. However, this did not happen because the current did not triple, as shown in Table II. The heat balance determines the electric power consumed. When the surface area tripled, the heat loss is also required to triple. However, the solution temperatures increased from 76 to 90 °C with the tripling of the surface area. If the solution temperature remains constant for each surface area, the production would have increased in proportion to the surface area. This result also suggested that cooling of the solution is essential to extend the plasma area.

F. Summary of the results

As mentioned in Secs. III A–III E, the key factors affecting the formation of nanoparticles are the current and voltage. The other factors such as solution temperature, electrolyte concentration, and surface area affect the current and voltage. For example, the solution temperature and surface area of the electrode just change the current. The high temperature caused a decrease in the current because the gas layer fully covered the electrode and prevented the flow of current. The voltage also affected the current and particle size. At high voltages,

the current decreased and the production increased. Low electrolyte concentration can increase the voltage, which probably causes sputtering of the electrode.

The role of the current is to control the amount of nanoparticles produced. Figure 9 shows the plot of current against the production rate. The shapes in the inset show the morphology of the electrode surface. This plot does not contain the t-1, t-5, V-80, and V-100 conditions because the amounts of nanoparticles produced in these cases were too small. The T-1 and T-2 conditions were also removed because a conventional electrolysis of water occurred at the interface between the electrode and the solution interface. From this plot, the current increased with the production rate because the current concentration produces a nanoparticle.

Figure 10 shows the plot of the mean diameter against the production density, i.e., the amount of nanoparticles produced per unit area. Interestingly, the surface morphologies affected the mean diameter and the production density. In addition, voltage changed the electrode surface. In the case of voltages below 140 V, the surfaces were either Particle or Ripple type. For voltages over 160 V, the surfaces changed to Random or Hole types, and these surfaces produced particles that were smaller than those produced from Ripple surfaces. The difference between Particle and Ripple type surfaces is in the production density; the production density was below 1.7 mg/cm² for Particle type surfaces and over

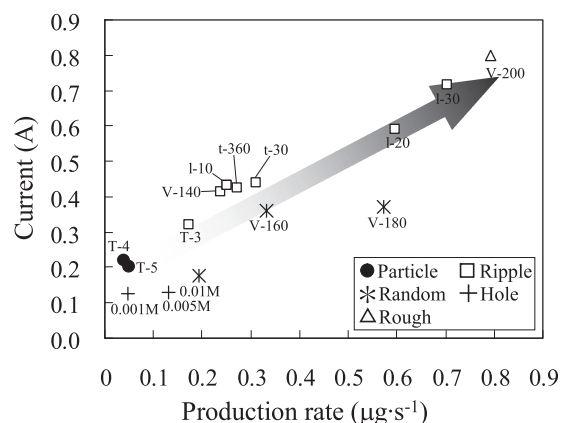


FIG. 9. Plot of mean current against the production rate. The inset shapes are a guide to the different morphologies of the electrode surface. The current increased with an increase in the production rate.

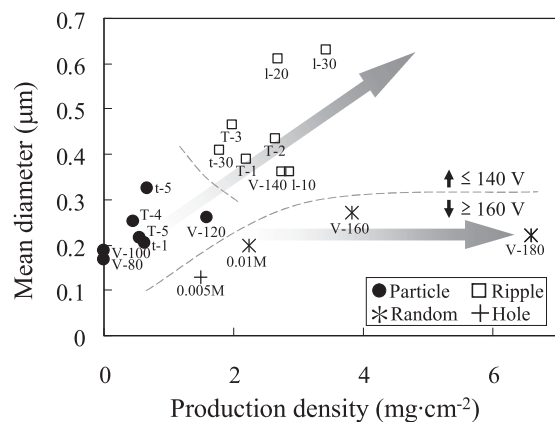


FIG. 10. Plot of the mean diameter against the production density. The inset shapes are a guide to the different morphologies of the electrode surface. The surface morphology affected the mean diameter and production density. The most suitable condition for the production of nanoparticles was the one in which the particle diameter was small and the production density was high. The Random type surface has a small diameter and high production density.

1.7 mg/cm² for Ripple type. Compared to Ripple surfaces, the Particle surfaces produced particles with a smaller diameter. The Particle surfaces probably change into Ripple surfaces during particle production. The spacing of the ripples became wider at a high production density, and the mean diameter increased with an increase in the production density. In contrast, the sizes of the particles produced from Random type surfaces were constant at different production densities.

G. Formation mechanism of nanoparticles

Previous reports indicate that the nanoparticles are produced via two mechanisms in the solution plasma: local melting of an electrode¹¹ because of the current concentration, which is induced by the electrothermal instability,^{20,21} and uniform sputtering in the form of a bombardment of charged particles in the plasma.^{2,22} In the case of ion beam sputtering, Xe⁺, Ar⁺, Kr⁺, and Ne⁺ ions have been used with an accelerating voltage of 1–60 kV. In the solution plasma, the main species in the plasma are OH⁻, Na⁺, H⁺, and ionized Ni.³ These ions seem to be too small to bombard the electrode surface. Additionally, the applied voltage of 140 V is relatively small, as compared to the ion beam irradiation. It is unlikely that nanoparticles formation during the glow discharge was induced by the ion sputtering process. Therefore, we consider that the local melting of an electrode produced nanoparticles. The current tends to concentrate in the pointed projection like a tip owing to the highly inhomogeneous electric field.²³ The surface morphology strongly affects the products size. Smooth and uniform surface, such as Particle and Random type, produces a small particle. When electrode surface grows to the Ripple and Rough type, the coarse particles are generated due to the inhomogeneous distribution of the current.

IV. CONCLUSION

In this study, we investigated the surface morphology of a glow discharge electrode in a solution. From these results, the morphologies of the electrodes were changed according to the experimental conditions. It was determined that the

current and voltage are the main factors. The following conclusions were drawn:

- (1) The production increased proportionally with electrolysis time and current.
- (2) When the voltages were below 140 V, surfaces with nanoparticles attached were formed on the electrode. These surfaces changed, and displayed ripples and the sizes of the particles produced increased with an increase in the production.
- (3) For voltages over 160 V, the surfaces of the electrodes were Random or Hole type, and the particle sizes were constant at different production densities.

In this study, we found a strong connection between the production and the electrode surface. These findings can help not only in the optimization of the experimental conditions but also in investigation of the formation mechanism of the nanoparticles in a solution plasma.

APPENDIX A: SUMMARY OF THE EXPERIMENTAL CONDITIONS

TABLE I. Experimental conditions. Samples with the same experimental conditions are denoted by asterisks.

Sample name	Time (min.)	Temperature Control	Maintained Voltage (V)	Electrolyte	Electrode Length (mm)
t-1	1	Natural	140	0.1 M NaOH	10
t-5	5	cooling in air			
t-30	30				
t-60 ^a	60				
t-360	360				
T-1	60	Quenched using ice water	140	0.1 M NaOH	410
T-2		Quenched using 25 °C water			
T-3 ^a		Natural cooling in air			
T-4		Heated using hotplate			
T-5		Strongly-heated using heater			
V-80	60	Natural cooling in air	80	0.1 M NaOH	10
V-100			100		
V-120			120		
V-140 ^a			140		
V-160			160		
V-180 ^b			180		
V-200			200		
0.001 M	60	Natural cooling in air	600	0.001 M NaOH	10
0.005 M			490	0.005 M NaOH	
0.01 M			400	0.01 M NaOH	
0.1 M ^b			180	0.1 M NaOH	
1.0 M			70	1.0 M NaOH	
I-10 ^a	60	Natural cooling in air	180	0.1 M NaOH	10
I-20			200		20
I-30					30

^aSame conditions.

^bSame conditions.

APPENDIX B: ANALYTICAL METHOD

In order to determine the mean diameter of the nanoparticles, four photographs of the spherical particles were taken for each experiment with the same magnification. From these four photographs, we measured the diameters of over 1000 particles whose diameters were greater than 10 nm. We calculated the volume mean diameter from this data. The volume mean diameter D_V differs from the number mean diameter D_n as shown by Eqs. (B1) and (B2). Here, the d_i stands for the diameter of particle i , and V_i mean the volume of the spherical particle with the diameter d_i .

$$D_n = \frac{\sum d_i}{n} \quad (\text{B1})$$

$$D_V = \frac{\sum (d_i \cdot V_i)}{\sum V_i} \quad (\text{B2})$$

We selected the volume mean diameter rather than number mean diameter because we could obtain a Gaussian distribution of the particle diameters by using a volume mean diameter.

The amount of nanoparticles produced (or Production) was calculated from the difference in the weight of the electrode before and after the experiments. We measured the electrode weight 5 times and calculated the average value. The nanoparticle production M (mg), production density d ($\text{mg}\cdot\text{cm}^{-2}$), and production rate v ($\text{mg}\cdot\text{s}^{-1}$) were derived by the equations listed below. Here, M_b is electrode weight before electrolysis and M_a is the weight after electrolysis. S is a surface area of the exposed part of the electrode, and t means the electrolysis time.

$$M = M_b - M_a \quad (\text{B3})$$

$$d = \frac{M_b - M_a}{S} \quad (\text{B4})$$

$$v = \frac{M_b - M_a}{t} \quad (\text{B5})$$

APPENDIX C: SUMMARY OF THE EXPERIMENTAL RESULTS

TABLE II. Experimental results. The breakdown voltage corresponds to the highest value of the current. The maintained current, power, and temperature are the average values during electrolysis. The production rate and density were derived by dividing the production by the electrolysis time and surface area, respectively.

Sample name	Breakdown				Maintained			Production (mg)	Particle size		
	Voltage (V)	Current (A)	Power (W)	Temp. ($^{\circ}\text{C}$)	Current (A)	Power (W)	Temp. ($^{\circ}\text{C}$)		N	Volume mean diameter (nm)	Number mean diameter (nm)
t-1	53.8	3.12	167	62.0	0.438	61.4	84.9	0.20	673	205	90
t-5	49.8	2.80	139	64.5	0.484	67.7	83.4	0.21	712	326	108
t-30	52.8	2.88	152	62.7	0.438	61.4	84.9	0.56	912	410	108
t-60	52.7	2.87	151	64.7	0.431	60.3	76.2	0.90	1950	361	113
t-360	50.8	2.76	140	64.3	0.424	59.3	69.2	5.86	777	439	119
T-1	71.9	2.54	183	48.8	0.991	138	64.3	0.69	842	389	115
T-2	60.9	1.86	113	53.0	0.606	84.8	68.5	0.83	1050	433	101
T-3	59.9	1.95	117	59.9	0.319	44.6	80.2	0.62	995	465	110
T-4	45.9	1.60	73.4	66.3	0.219	30.7	92.0	0.14	1005	253	104
T-5	43.9	1.21	53.1	65.4	0.200	28.0	99.1	0.18	1384	215	102
V-80	49.8	2.78	138	63.4	0.831	66.4	87.4	0.01	1076	168	61
V-100	52.8	2.59	137	60.1	0.593	59.3	85.9	0.01	664	187	61
V-120	51.8	2.90	150	62.3	0.503	60.3	84.2	0.50	796	261	87
V-140	51.8	2.74	142	64.5	0.413	57.8	85.3	0.86	1950	361	113
V-160	51.8	2.74	142	64.9	0.360	57.6	83.6	1.20	501	271	102
V-180	51.8	2.76	143	60.1	0.371	66.7	81.3	2.07	1257	222	61
V-200	46.6	2.99	139	63.7	0.801	160	93.3	2.85	921	380	133
0.001 M	479	0.40	192	74.3	0.125	75.3	87.8	0.17	–	–	–
0.005 M	275	0.63	174	67.7	0.130	63.8	85.8	0.47	2072	129	56
0.01 M	176	0.99	174	72.5	0.176	70.2	85.6	0.70	465	198	77
0.1M	79.8	0.87	69.4	68.2	0.371	66.7	81.3	2.07	1257	222	61
1.0M	21.5	2.91	62.6	62.7	0.544	38.1	73.2	0.32	–	–	–
l-10	51.8	2.74	142	64.5	0.431	60.3	76.2	0.90	1950	361	113
l-20	53.8	4.94	266	65.2	0.590	82.5	89.0	2.15	1210	630	66
l-30	55.8	6.86	383	61.4	0.718	100	89.7	2.53	837	611	120

- ¹A. Hickling and M. Ingram, *J. Electroanal. Chem.* **8**, 65 (1964).
- ²K. Azumi, A. Kanada, M. Kawaguchi, and M. Seo, *Hyomen Gijutsu* **56**, 938 (2005).
- ³K. Azumi, T. Mizuno, T. Akimoto, and T. Ohmori, *J. Electrochem. Soc.* **146**, 3374 (1999).
- ⁴K. Kobayashi, Y. Tomita, and M. Sanmyo, *J. Phys. Chem. B* **104**, 6318 (2000).
- ⁵J. Gao, A. Wang, Y. Li, Y. Fu, J. Wu, Y. Wang, and Y. Wang, *React. Funct. Polym* **68**, 1377 (2008).
- ⁶J. Gong, J. Wang, W. Xie, and W. Cai, *J. Appl. Electrochem.* **38**, 1749 (2008).
- ⁷T. Kareem and A. Kaliani, *Ionics* **18**, 315 (2012).
- ⁸M. A. Bratescu, S.-P. Cho, O. Takai, and N. Saito, *J. Phys. Chem. C* **115**, 24569 (2011).
- ⁹S. M. Kim, G. S. Kim, and S. Y. Lee, *Mater. Lett.* **62**, 4354 (2008).
- ¹⁰T. Paulmier, J. M. Bell, and P. M. Fredericks, *J. Mater. Process. Technol.* **208**, 117 (2008).
- ¹¹Y. Toriyabe, S. Watanabe, S. Yatsu, T. Shibayama, and T. Mizuno, *Appl. Phys. Lett.* **91**, 041501 (2007).
- ¹²G. Saito, S. Hosokai, and T. Akiyama, *Mater. Chem. Phys.* **130**, 79 (2011).
- ¹³G. Saito, S. Hosokai, M. Tsubota, and T. Akiyama, *J. Appl. Phys.* **110**, 023302 (2011).
- ¹⁴G. Saito, S. Hosokai, T. Akiyama, S. Yoshida, S. Yatsu, and S. Watanabe, *J. Phys. Soc. Jpn* **79**, 083501 (2010).
- ¹⁵G. Saito, S. Hosokai, M. Tsubota, and T. Akiyama, *Plasma Chem. Plasma Process.* **31**, 719 (2011).
- ¹⁶J. Roth, J. Rahel, X. Dai, and D. Sherman, *J. Phys. D: Appl. Phys.* **38**, 555 (2005).
- ¹⁷M. Tokushige, T. Nishikiori, and Y. Ito, *J. Electrochem. Soc.* **157**, E162 (2010).
- ¹⁸M. Tokushige, T. Nishikiori, and Y. Ito, *Russ. J. Electrochem.* **46**, 619 (2010).
- ¹⁹C. Cho, Y. Choi, C. Kang, and G. Lee, *Appl. Phys. Lett.* **91**, 141501 (2007).
- ²⁰R. Uncles and A. Nelson, *Plasma Phys.* **12**, 917 (1970).
- ²¹K. Okazaki, Y. Mori, K. Hijikata, and K. Ohtake, *AIAA J.* **16**, 334 (1978).
- ²²K. Azumi, A. Kanada, M. Seo, and T. Mizuno, *Electrochim. Acta* **52**, 4463 (2007).
- ²³W. G. Graham and K. R. Stalder, *J. Phys. D: Appl. Phys.* **44**, 174037 (2011).
- ²⁴See supplementary material at <http://dx.doi.org/10.1063/1.4732076> for detailed experimental results, including the SEM images of the electrode surface, TEM image of the particles, XRD pattern of the products, and the power requirements for plasma generation.